

High order Brunel harmonics and supercontinuum formed by a weak optical pump in presence of a strong terahertz field

I. Babushkin,^{1,2,3} A. Demircan,^{1,2} U. Morgner,^{1,2} and A. Savel'ev^{4,5}

¹*Institute for Quantum Optics, Leibniz Universität Hannover, Welfengarten 1, 30167 Hannover, Germany*

²*Cluster of Excellence PhoenixD (Photonics, Optics, and Engineering – Innovation Across Disciplines), Welfengarten 1, 30167 Hannover, Germany*

³*Max Born Institute, Max Born Str. 2a, 12489 Berlin, Germany*

⁴*Faculty of Physics, Lomonosov Moscow State University, Leninskie gory, 2 119991, Moscow, Russia*

⁵*Lebedev Physical Institute Russian Academy of Sciences, Leninskii prosp. 53, 119991, Moscow, Russia*

Brunel harmonics appear in the optical response of an atom in process of laser-induced ionization, when the electron leaves the atom and is accelerated in the strong optical field. In contrast to recollision-based harmonics, the Brunel mechanism does not require the electron returning to the core. Here we show that in the presence of a strong ionizing terahertz (THz) field, even a weak driving field at the optical frequencies allow for generating Brunel harmonics effectively. The strong ionizing THz pump suppresses recollisions, making Brunel dominant in a wide spectral range. High-order Brunel harmonics may form a coherent carrier-envelope-phase insensitive supercontinuum, compressible into an isolated pulse with the duration down to 100 attoseconds.

Introduction. As it has been known from early stage of laser optics, interaction of a strong optical field at frequency ω_0 with matter creates harmonics at $n\omega_0$, taking place via virtual bound-bound atomic/molecular transitions [1]. Much later it was discovered that for higher intensities, when the atoms and molecules are ionized, high-harmonic generation (HHG) appears due to the subsequent return of electrons to their parent cores [2], leading to birth of attosecond science [3] and allowing to break the femtosecond boundary for the pulse duration possessed by previous techniques [3, 4].

It was realized nearly at the same time that electron creation during ionization in a strong field also leads to appearance of harmonics [5] via bound-free and free-free transitions, that is, without need of the electron to come back. Here, following [6, 7] we will call the corresponding nonlinearity “Brunel nonlinearity” and the arising harmonics will be denoted as “Brunel harmonics”. The ionization-induced nonlinearities are typically “nonperturbative”, that is, one can not obtain the harmonics as series expansion in the vicinity of zero driver field – in contrast to a typical case of nonresonant bound-bound nonlinearities. This is related to the fact that Brunel harmonics are proportional to the free electron density which, in turns, grows exponentially fast with the field in the tunnel ionization regime [8].

Brunel nonlinearity has been found to be useful, in particular, for generation of low-frequency harmonics, in the terahertz (THz) domain [9, 10]. The efficiency of such scheme for THz generation can compete with optical rectification in crystals [11, 12]. More generally, generation of high-amplitude THz radiation opens wide new perspectives [13], from remote detection for biological applications [10] to compact electron accelerators [14].

Studies of the extreme-field THz interaction with matter are currently in their infancy due to quite a few

available sources of extreme THz fields. Some work in this direction was also done before, by exploring the influence of a “strong” DC or quasi-DC field on high harmonic generation (HHG) by an optical field [15] and on generation of attosecond pulses [16]. This situation is changing currently, in particular, due to novel sources of extreme THz fields exceeding 100 MV/cm level [17, 18], allowing to consider processes appearing in the extreme-field regime at THz frequencies [19], such as generation of high harmonics of the THz field [20]. In [21] it was shown that HHG from the intense mid-infrared (IR) field (670 MV/cm) can be controlled efficiently with a strong THz field (100 MV/cm at 33 THz). Here the optical field was high enough for tunnel ionization of Ne atoms, while the THz field modified (not too significantly) the ionized electrons paths, being not high enough to cause ionization.

The limit, where the THz field can ionize atoms/molecules/solids directly, is of special interest since achievable THz field strengths exceed greatly the DC breaking threshold of a medium [22, 23]. In particular, impact-ionization-induced transient optical nonlinearity was considered recently in *p*-Si at THz field above 10 MV/cm [24].

In this paper, we consider HHG created by a weak probe pulse at optical (in particular mid-IR) frequencies, in the presence of an extreme THz transient with intensity slightly below the onset of the tunnel ionization. We show that the weak optical probe triggers tunnel ionization on the subcycle scale, leading to a strong nonlinear response of atoms governed by the Brunel mechanism. We observe that the strong THz driver suppresses recollision-based harmonics, making the Brunel nonlinearity dominant. When the optical probe has a few-cycle duration, the Brunel harmonics form a broad coherent supercontinuum with a flat spectral phase profile, independent on the carrier-

envelope phase, capable of compression to an isolated attosecond-scale pulse.

Simple-man picture. To start with, we formulate our idea using a simple-man quasi-static tunnel-based model of the ionization in strong optical fields [8]. In this framework, the electron tunnels from the ground state to the continuum through the barrier, created, on the one side, by the core potential, and on the other side, by the strong external driving field (see Fig. 1a). Effectively the electron can be considered as being born in continuum with ionization rate $W(t) = (\alpha/|\mathbf{E}|) \exp(-\beta/|\mathbf{E}|)$, where α and β are some coefficients and \mathbf{E} is the driving field strength [8]. The free electrons form a current [7, 25, 26] given, under the assumption that the initial velocity is negligible, by (here and thereafter we use Hartree atomic units):

$$\frac{d\mathbf{J}}{dt} = \rho(t)\mathbf{E}(t). \quad (1)$$

Here $W(t)$ and the free electron density $\rho(t)$ are connected by $\frac{d\rho(t)}{dt} = W(t)(\rho_0(t) - \rho(t))$, where $\rho_0(t)$ is the density of neutrals before the field is switched on.

The change of the current, according to the Maxwell equations, serves as a source of electromagnetic radiation $\mathbf{E}_r \propto d\mathbf{J}/dt$, which is here referred to as Brunel harmonics. When the initial driving pulse is a strong THz wave with intensity just below the onset of the tunnel ionization, the presence of even a weak pulse at the optical frequency, leads to a significant modulation of the tunneling probability at the subcycle scale, and thus to a strong nonlinear response (see inset to Fig. 1a). An exemplary simulation is shown in Fig. 1, where Fig. 1a shows the dynamics of the ionization of an argon atom for the case of the pump given by the linearly polarized THz field of duration of 100 fs, central frequency 3 THz and amplitude $E_{\text{THz}} = 0.03$ a.u. (156 MV/cm), whereas the optical driver has a linear polarization, co-directed with the THz field, with 10 fs duration and field amplitude $E_{\text{opt}} = 0.012$ a.u. (60 MV/cm), centered at 800 nm wavelength. In Fig. 1b the corresponding spectrum is shown for this pump configuration by the blue line. As one can see by the comparison to the case of the same E_{opt} but zero E_{THz} (green dashed line in Fig. 1b), the presence of a strong THz pump leads to a significant amplification of the Brunel nonlinearity and thus of the intensity of the Brunel harmonics. The inset to Fig. 1b also shows that this intensity grows quickly with increasing of E_{opt} . We see also that the Brunel harmonics decay exponentially with the harmonics number, as it is known also for other pump configurations [27]. Nevertheless, harmonics up to order ~ 10 are yet quite pronounced. In contrast to a single-pump configuration, both even and odd harmonics are present. This is the obvious consequence of the fact that the THz wave breaks the inversion symmetry of the whole system. Also, for the sake of comparison, in Fig. 1b (black dashed line) we

plotted Brunel harmonics given by the purely optical field $E_{\text{opt}} = 0.042$ a.u., corresponding to $E_{\text{THz}} + E_{\text{opt}}$ in the previous configuration. One can see that also for the odd harmonics of relatively low order (below $n \sim 5$), our two-color configuration provides an advantage in efficiency over the single-color one. As we see in the next session by considering a more detailed picture, Brunel harmonics in the single color configuration have no advantage also for higher frequencies $n \gtrsim 5$.

Quantum-mechanical approach. As a next step, we simulate the ionization process using the time-dependent Schrödinger equation (TDSE) for the hydrogen atom:

$$i\partial_t\psi(\mathbf{r}, t) = H\psi(\mathbf{r}, t), \quad H = (\mathbf{p} + \mathbf{A}(t))^2/2 + V(r), \quad (2)$$

where $\psi(\mathbf{r}, t)$ is the wavefunction of the electron depending on space \mathbf{r} (with $r \equiv |\mathbf{r}|$) and time t coordinates, H is the electron's Hamiltonian, with \mathbf{p} being the momentum operator, $\mathbf{A}(t)$ the vector potential of the driving field corresponding to the electric field strength $\mathbf{E}(t) = -\partial_t\mathbf{A}$, and $V = -1/r$ is the potential created by the hydrogen core. The optical response of the atom, which in this case includes not only Brunel mechanism but also bound-bound transitions and recollision harmonics, is given by

$$\mathbf{E}_r = \frac{d^2}{dt^2} \langle \psi | \mathbf{r} | \psi \rangle. \quad (3)$$

The code developed in [28] was used to perform the numerical integration, with the simulation box size of 500 a.u.. The driving field was given by $\mathbf{A} = \mathbf{A}_{\text{THz}} + \mathbf{A}_{\text{opt}}$,

$$A_{x,\text{opt}} = e^{-\frac{t^2}{\tau_{\text{opt}}^2}} \sin(\omega_0 t), \quad A_{x,\text{THz}} = e^{-\frac{t^2}{\tau_{\text{THz}}^2}} \sin(\omega_{\text{THz}} t), \quad (4)$$

and $A_{y,\text{opt}} = 0$, $A_{y,\text{THz}} = 0$, where ω_0 is frequency corresponding to 800 nm wavelength and $\omega_{\text{THz}} = 3 \times 2\pi$ THz, τ_{opt} corresponds to 5 fs full-width half-maximum (FWHM) and τ_{THz} corresponding to 100 fs FWHM pulse durations.

The simulation results are shown in Fig. 2a,b for E_{THz} and E_{opt} the same as in Fig. 1a. In Fig. 2a, the spectrum of \mathbf{E}_r (for two different carrier-envelope (CEO) phases, 0 and π , and in (b) the XFROG trace for the zero CEO phase is presented. For comparison, in Fig. 2c,d the same pictures are shown for the strong optical pump only (equal to the sum of E_{opt} and E_{THz} from the previous case). As one can see, in the latter case high order harmonics up to ~ 17 appear. Examining the XFROG Fig. 2d we see that these harmonics originate from the recollision harmonics. Indications of this is the characteristic time-dependent delay in harmonic emission visible in Fig. 2d. In contrast, in the former case of THz+optical pump the harmonics have no systematic delay, pointing to the Brunel generation mechanism. We see also that the harmonics are less localized in time in the two-color case, which is also good explained by

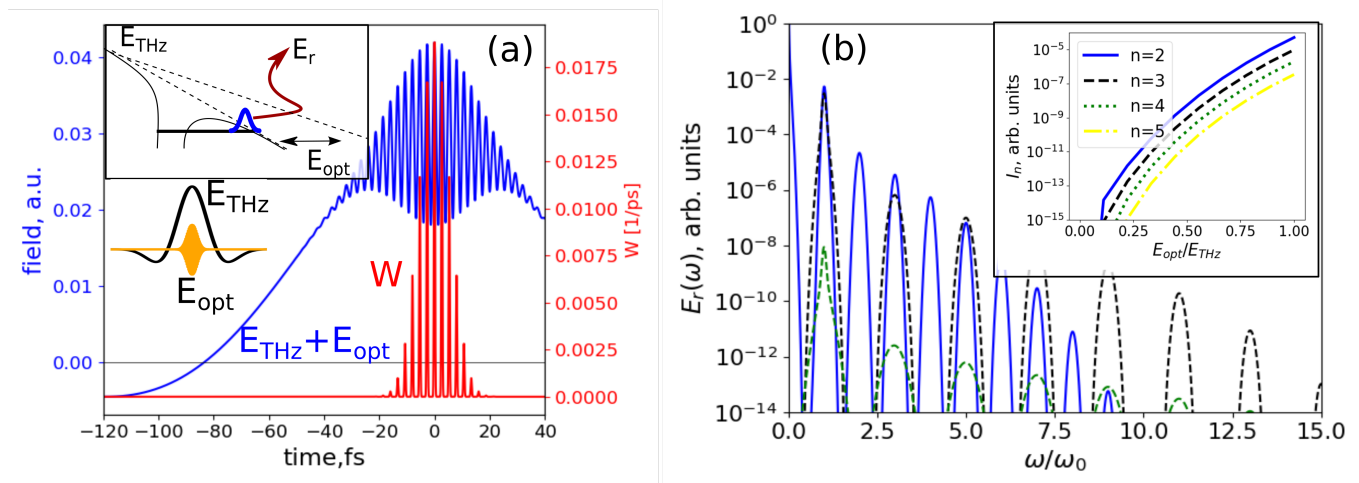


FIG. 1. Nonlinear response of argon to a weak optical probe pulse in presence of a strong THz field – a simple-man picture. (a) Exemplary electric field (blue line) consisting of a strong THz ($E_{\text{THz}} = 0.03$ a.u.) centered at $100 \mu\text{m}$ wavelength and a weaker fundamental harmonic at 800 nm wavelength ($E_{\text{opt}} = 0.012$ a.u.), together with the ionization rate $W(t)$ (red line) induced by such a waveshape in argon according to the tunnel model. The lower inset shows the composition of the full driver signal from strong THz E_{THz} and weak optical E_{opt} field. The upper inset shows the schematics of the basic mechanism. (b) Corresponding Brunel harmonic response as given by Eq. (1) (blue line). For comparison, also the Brunel harmonics created by the optical field alone with the amplitude $E_{\text{opt}} = 0.042$ a.u. (corresponding to $E_{\text{opt}} + E_{\text{THz}}$ from (a), black dashed line) and $E_{\text{opt}} = 0.012$ a.u. (corresponding to E_{opt} from (a), green dashed line). The latter is multiplied by 10^{35} for better visibility. The inset shows the intensity of n th harmonics (for several values of n) in dependence on E_{opt} .

the Brunel mechanism, since Brunel harmonics are born in the process of both electron birth and acceleration, so their generation should take certain time. The different generation mechanism is furthermore indicated by radically different spectral phases for two- and single-color cases, shown by the black lines in Fig. 2a and Fig. 2d. The former is almost frequency independent, in strong contrast to the latter. The spectrum in the two-color case is extended only up to around 10th harmonic in a qualitative agreement with the simple-man theory (see Fig. 1b), also supporting the Brunel mechanism for that case.

This suggests, that recollision-based harmonics are significantly suppressed. To obtain an additional confirmation of this suppression, we made simulations of one-dimensional variant of Eq. (2) with a soft-core Coulomb potential $V = -1/\sqrt{x^2 + a^2}$, which, for $a = 1/\sqrt{2}$ has the same ionization potential as the hydrogen atom [29, 30]. The results of simulation for the same parameters of as in Fig. 2a and Fig. 2d are given in Fig. 2c and Fig. 2f respectively. The advantage of the one-dimensional simulation is that one can very clearly see the trajectories of the electrons: If the strong THz field is present (Fig. 2c), the electrons move from the core without making even a single recollision, in a strong contrast to the case of the single color optical pump (Fig. 2f). This is explained by the fact that the ponderomotive energy gained by the electron from the THz field over the half of the optical field cycle $\propto E_{\text{THz}}^2$ which is in our case one order of magnitude larger than

the energy gained from the optical field $\propto E_{\text{opt}}^2$ over the same time. Because the subsequent optical half-cycles are located within the very same THz cycle, the electron do have no chances to return back.

Importantly, the spectrum in Fig. 2a forms a broad continuum in the range of $n \approx 1.5 - 10$ harmonics. The most important reason why separate harmonics join into a broad continuum is rather the short optical probe, leading to broadening of every harmonic; Besides, in our case both odd and even harmonics are present, so the distance between the subsequent harmonics is two times smaller than in a single-color case. The spectral phase of the resulting continuum is very flat across the whole spectral range (see black line in Fig. 2a); Removing this phase leads to a stand-alone Fourier-limited compressed pulse of a 100-attosecond duration as shown in Fig. 3. If the spectral range from 1.5th to 10th harmonic is taken for compression, the resulting pulse is 120 attoseconds long, whereas if the whole spectrum above 1.5th harmonic is used, the final pulse duration is reduced to 85 attoseconds.

Very importantly, both the spectral intensity and the spectral phase are rather insensitive to the CEO phase of the optical probe (see Fig. 2a, where the cases of different CEO phases are shown by solid and dashed lines). This is in a strong contrast to the continua created by recollision-based harmonics (which are also located at higher frequencies) [31–33]. These continua are heavily CEO-dependent since they rely on the inter-cycle electrons trajectories leading back

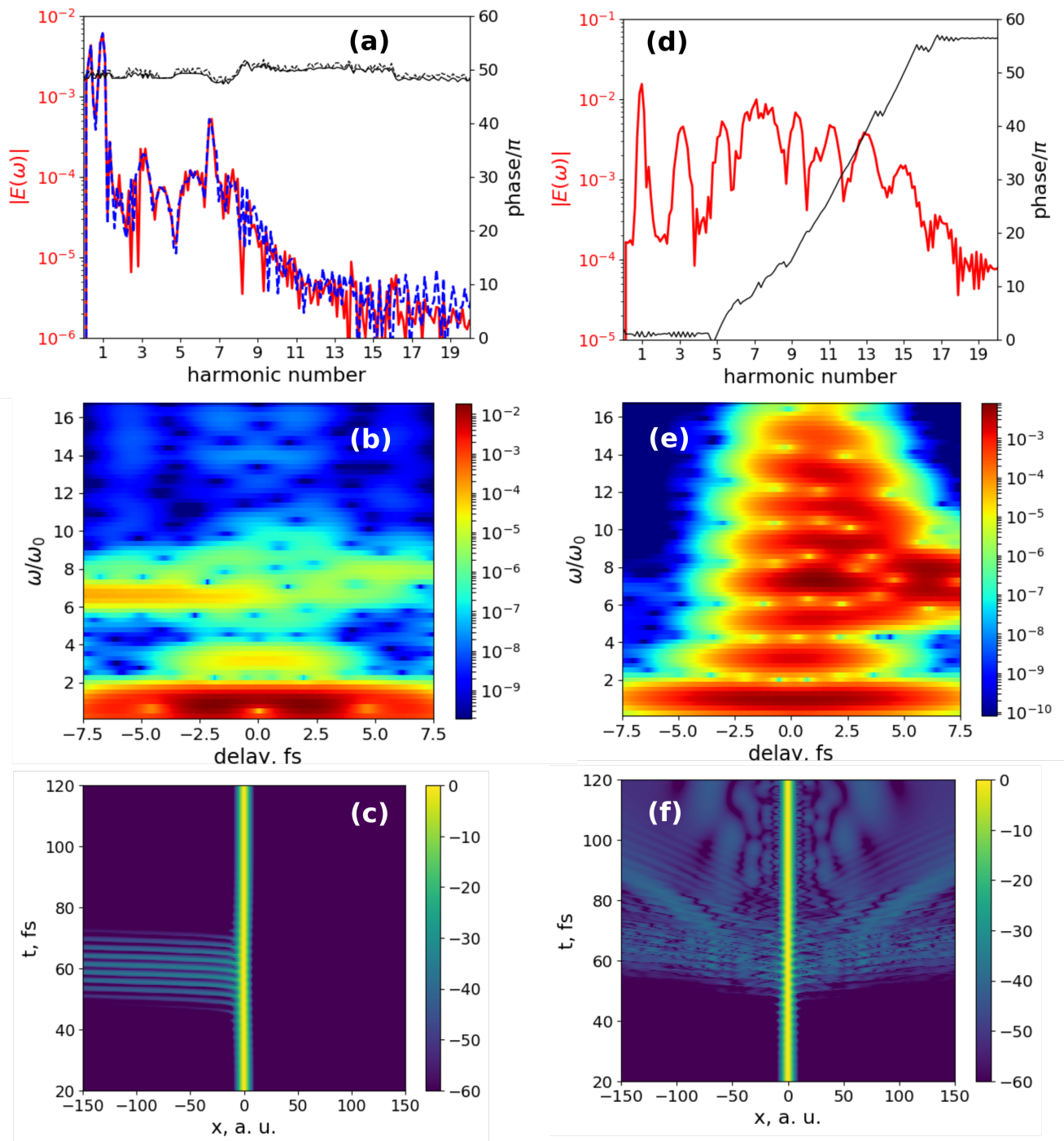


FIG. 2. The response of the hydrogen atom according to TDSE simulations [Eq. (2)] with E_{opt} given by a 5 fs-long pulse with (a,b,c) and without (e,d,f) a strong THz field. The field amplitudes are as in Fig. 1. (a,c) The harmonic spectrum of the atomic response \mathbf{E}_r , according to Eq. (3). Red and blue lines: spectral amplitudes, black lines: spectral phases. In (a), the cases of the CEO phase = 0 (solid lines) and π (dashed lines) are shown. (b,d) Corresponding XFROG traces. (e,f) Spatio-temporal dynamics of the electron wavepacket $|\psi(x,t)|^2$ simulated by 1D-variant of Eq. (2) with a regularized Coulomb potential (see text).

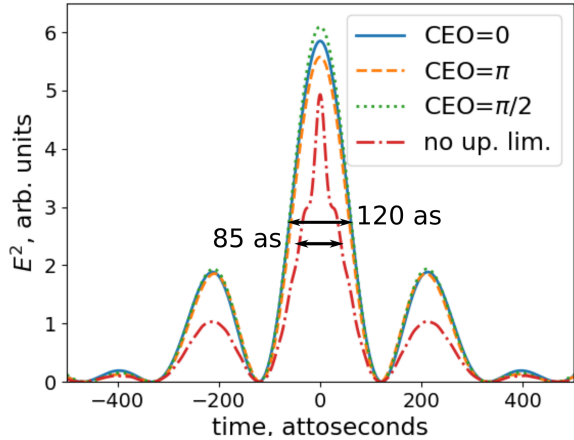


FIG. 3. Solid blue line: The square of the electric field in dependence on time for the Fourier-limited pulse obtained from the spectrum spectrum in in Fig. 2a in the range between $\omega = 1.5\omega_0$ and $\omega = 10\omega_0$. FWHM duration of the resulting pulse is 120 attoseconds. To demonstrate the CEO-insensitivity, dashed orange and dotted green lines show the cases of the different CEO phase of the optical driver, compressed with the phase mask for the zero CEO phase. Red dash-dotted line shows the compressed pulse with the same lower but with no upper filtering limit. In this case FWHM duration is 85 fs.

to the core. In contrast, the Brunel radiation is emitted during the ionization event, taking place on the subcycle scales. Interestingly, the CEO-insensitivity of the continuum is also rather different from the behaviour of separate harmonics obtained from longer pump pulses (for instance in Fig. 1b) where the CEO phase of n th harmonic is n times the CEO phase of the fundamental. This pronounced CEO-insensitivity leads also to the insensitivity of the resulting compressed pulse to the CEO phase, as shown in Fig. 3 where compression of spectra resulted from optical probe with different CEO phases is made using the same phase mask. That is, the compression scheme does not require CEO stabilization of the optical probe. As we see, these pulses do not require also gating necessary for isolating attosecond pulses for recollision-based harmonics [31–33].

Conclusion and discussions. In conclusion, we showed that in the presence of a strong ionizing THz driver, higher order harmonics can be generated by a weak optical probe pulse via the Brunel (ionization-induced) mechanism. This mechanism dominates over recollision-based harmonics, since the recollisions are strongly suppressed in the presence of the strong THz wave. When generated with a few-cycle optical pump, the harmonics in the range from visible to XUV may form a broadband supercontinuum, compressible to an isolated 100-attosecond-scale pulse without need for gating techniques. The generation efficiency is

comparable to the one based on recollision harmonics, but taking into account that the spatial area of focused THz pulses is around four orders of magnitude larger than the area at optical frequencies, and, since only a weak optical driver is needed (which thus can be significantly defocused), the overall energy yield can be several orders of magnitude higher than from the recollision-based mechanism.

Importantly, this approach is fully insensitive to the CEO phase of the optical driver, so that CEO stabilization is not required. CEO-phase-insensitivity implies also shot-to-shot coherence of the supercontinuum, the property which is difficult to achieve using traditional fiber-based supercontinuum generation methods [34–36].

A.S. acknowledges support from the Russian Science Foundation under project 20-19-00148. I.B. and U.M. thank Deutsche Forschungsgemeinschaft (DFG, German Research Foundation), projects BA 4156/4-2 and MO 850-19/2 for support. I.B., A.D. and U.M. acknowledge support from Germany’s Excellence Strategy within the Cluster of Excellence PhoenixD (EXC 2122, Project ID 390833453).

-
- [1] R. W. Boyd, *Nonlinear Optics* (Academic Press, Amsterdam, 2008).
 - [2] P. B. Corkum, N. H. Burnett, and F. Brunel, Above-threshold ionization in the long-wavelength limit, *Phys. Rev. Lett.* **62**, 1259 (1989).
 - [3] P. B. Corkum and F. Krausz, Attosecond science, *Nat. Phys.* **3**, 381 (2007).
 - [4] P. B. Corkum, N. H. Burnett, and M. Y. Ivanov, Subfemtosecond pulses, *Opt. Lett.* **19**, 1870 (1994).
 - [5] F. Brunel, Harmonic generation due to plasma effects in a gas undergoing multiphoton ionization in the high-intensity limit, *J. Opt. Soc. Am. B* **7**, 521 (1990).
 - [6] T. Balčiūnas, D. Lorenc, M. Ivanov, O. Smirnova, A. Zheltikov, D. Dietze, K. Unterrainer, T. Rathje, G. Paulus, A. Baltuška, *et al.*, CEP-stable tunable THz-emission originating from laser-waveform-controlled sub-cycle plasma-electron bursts, *Opt. Express* **23**, 15278 (2015).
 - [7] I. Babushkin, C. Brée, C. M. Dietrich, A. Demircan, U. Morgner, and A. Husakou, Terahertz and higher-order Brunel harmonics: from tunnel to multiphoton ionization regime in tailored fields, *J. Mod. Opt.* **64**, 1078 (2017).
 - [8] L. Keldysh *et al.*, Ionization in the field of a strong electromagnetic wave, *Sov. Phys. JETP* **20**, 1307 (1965).
 - [9] T. Bartel, P. Gaal, K. Reimann, M. Woerner, and T. Elsaesser, Generation of single-cycle THz transients with high electric-field amplitudes, *Opt. Lett.* **30**, 2805 (2005).
 - [10] K. Reimann, Terahertz radiation: A table-top source of strong pulses, *Nat. Photonics* **2**, 596 (2008).
 - [11] K.-L. Yeh, M. C. Hoffmann, J. Hebling, and K. A. Nelson, Generation of 10 μ J ultrashort terahertz pulses by optical rectification, *Appl. Phys. Lett.* **90** (2007).

- [12] J. A. Fülöp, L. Pálfalvi, S. Klingebiel, G. Almási, F. Krausz, S. Karsch, and J. Hebling, Generation of sub-mj terahertz pulses by optical rectification, *Opt. Lett.* **37**, 557 (2012).
- [13] S. Dhillon, M. Vitiello, E. Linfield, A. Davies, M. C. Hoffmann, J. Booske, C. Paoloni, M. Gensch, P. Weightman, G. Williams, *et al.*, The 2017 terahertz science and technology roadmap, *J. Phys. D: Appl. Phys.* **50**, 043001 (2017).
- [14] E. A. Nanni, W. R. Huang, K.-H. Hong, K. Ravi, A. Fallahi, G. Moriena, R. D. Miller, and F. X. Kärtner, Terahertz-driven linear electron acceleration, *Nat. Commun.* **6**, 1 (2015).
- [15] M.-Q. Bao and A. F. Starace, Static-electric-field effects on high harmonic generation, *Phys. Rev. A* **53**, R3723 (1996).
- [16] Y. Pan, S.-F. Zhao, and X.-X. Zhou, Generation of isolated sub-40-as pulses from gas-phase co molecules using an intense few-cycle chirped laser and a unipolar pulse, *Phys. Rev. A* **87**, 035805 (2013).
- [17] C. Vicario, B. Monoszlai, and C. P. Hauri, GV/m single-cycle terahertz fields from a laser-driven large-size partitioned organic crystal, *Phys. Rev. Lett.* **112**, 213901 (2014).
- [18] A. Sell, A. Leitenstorfer, and R. Huber, Phase-locked generation and field-resolved detection of widely tunable terahertz pulses with amplitudes exceeding 100 mv/cm, *Opt. Lett.* **33**, 2767 (2008).
- [19] X. C. Zhang, A. Shkurinov, and Y. Zhang, Extreme terahertz science, *Nat. Photonics* **11**, 16 (2017).
- [20] O. Schubert, M. Hohenleutner, F. Langer, B. Urbanek, C. Lange, U. Huttner, D. Golde, T. Meier, M. Kira, S. W. Koch, *et al.*, Sub-cycle control of terahertz high-harmonic generation by dynamical bloch oscillations, *Nat. Photonics* **8**, 119 (2014).
- [21] E. Balogh, K. Kovacs, P. Dombi, J. A. Fulop, G. Farkas, J. Hebling, V. Tosa, and K. Varju, Single attosecond pulse from terahertz-assisted high-order harmonic generation, *Phys. Rev. A* **84**, 023806 (2011).
- [22] O. Chefonov, A. Ovchinnikov, S. Romashevskiy, X. Chai, T. Ozaki, A. Savel'ev, M. Agranat, and V. Fortov, Giant self-induced transparency of intense few-cycle terahertz pulses in n-doped silicon, *Opt. Lett.* **42**, 4889 (2017).
- [23] O. V. Chefonov, A. V. Ovchinnikov, M. B. Agranat, V. E. Fortov, E. S. Efimenko, A. N. Stepanov, and A. B. Savel'ev, Nonlinear transfer of an intense few-cycle terahertz pulse through opaque n-doped Si, *Phys. Rev. B* **98**, 165206 (2018).
- [24] A. Savel'ev, O. Chefonov, A. Ovchinnikov, A. Rubtsov, A. Shkurinov, Y. Zhu, M. Agranat, and V. Fortov, Transient optical non-linearity in p-Si induced by a few cycle extreme THz field, *Opt. Express* **29**, 5730 (2021).
- [25] K.-Y. Kim, Generation of coherent terahertz radiation in ultrafast laser-gas interactions, *Phys. Plasmas* **16**, 056706 (2009).
- [26] I. Babushkin, S. Skupin, and J. Herrmann, Generation of terahertz radiation from ionizing two-color laser pulses in Ar filled metallic hollow waveguides, *Opt. Express* **18**, 9658 (2010).
- [27] I. Babushkin, S. Skupin, A. Husakou, C. Köhler, E. Cabrera-Granado, L. Bergé, and J. Herrmann, Tailoring terahertz radiation by controlling tunnel photoionization events in gases, *New J. Phys* **13**, 123029 (2011).
- [28] S. Patchkovskii and H. Muller, Simple, accurate, and efficient implementation of 1-electron atomic time-dependent schrödinger equation in spherical coordinates, *Computer Physics Communications* **199**, 153 (2016).
- [29] J. H. Eberly, Q. Su, and J. Javanainen, Nonlinear light scattering accompanying multiphoton ionization, *Phys. Rev. Lett.* **62**, 881 (1989).
- [30] R. L. Hall, N. Saad, K. D. Sen, and H. Ciftci, Energies and wave functions for a soft-core coulomb potential, *Phys. Rev. A* **80**, 032507 (2009).
- [31] I. P. Christov, M. M. Murnane, and H. C. Kapteyn, High-harmonic generation of attosecond pulses in the "single-cycle" regime, *Phys. Rev. Lett.* **78**, 1251 (1997).
- [32] T. Brabec and F. Krausz, Intense few-cycle laser fields: Frontiers of nonlinear optics, *Rev. Mod. Phys.* **72**, 545 (2000).
- [33] M. Chini, K. Zhao, and Z. Chang, The generation, characterization and applications of broadband isolated attosecond pulses, *Nat. Photonics* **8**, 178 (2014).
- [34] A. Demircan and U. Bandelow, Supercontinuum generation by the modulation instability, *Opt. Comm.* **244**, 181 (2005).
- [35] J. M. Dudley, G. Genty, and S. Coen, Supercontinuum generation in photonic crystal fiber, *Rev. Mod. Phys.* **78**, 1135 (2006).
- [36] I. Babushkin, A. Tajalli, H. Sayinc, U. Morgner, G. Steinmeyer, and A. Demircan, Simple route toward efficient frequency conversion for generation of fully coherent supercontinua in the mid-IR and UV range, *Light Sci. Appl.* **6**, e16218 (2017).